

Supplementary material to “On the rheology of pendular gels and morphological developments in paste-like ternary systems based on capillary attraction”

Trystan Domenech and Sachin Velankar

Elastic to plastic transition and yielding under dynamic shear

The complex moduli of the binary and ternary blends for $\phi_{SP} = 0.2$ are represented as a function of oscillatory stress amplitudes in Fig. S1a. Unlike the PIB/SP system, the ternary blend exhibits a sharp

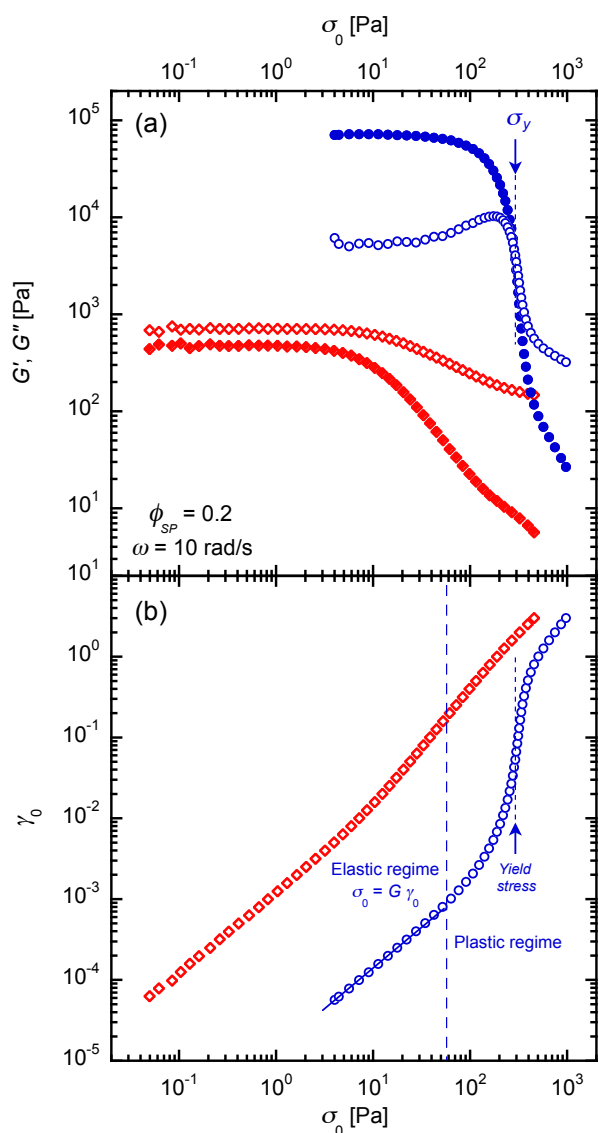


Fig. S1 (a) Complex moduli (G' : filled symbols, G'' : open symbols) and (b) strain amplitude vs. stress amplitude during dynamic strain sweeps for PIB/SP ($\varrho = 0$, red symbols) and PIB/PEO/SP ($\varrho = 0.16$, blue symbols) blends with $\phi_{SP} = 0.2$.

decrease in G' marked by a $G' - G''$ crossover. This solid-to-fluid transition happens for an oscillatory stress amplitude corresponding to the yield stress σ_y , which is found to be very close to the yield stress measured in steady state flow conditions (Fig. 8a).

When these data are plotted in terms of stress-strain amplitudes, typical elastic to plastic transition is observed for the ternary system (see Fig. S1b). The elastic regime corresponds to the linear viscoelastic domain (where $\sigma_0 = G\gamma_0$ with $G \approx G'_p$), whereas plastic behavior appears in the nonlinear domain (with the yield stress corresponding to the oscillatory stress at the inflection point of the stress-strain curve as shown in Fig. S1b).

Morphological observations of the ternary blends in the pendular regime

Pendular systems were observed by optical microscopy for a particle volume fraction spanning from 0.01 to 0.25. The DIC micrographs are shown in Fig. S2. Isolated pendular flocs, which are typically observed for $\phi_{SP} < 0.046$, are highlighted by the white dashed ellipses.

Rheology of PIB/SP binary blends

The linear and nonlinear viscoelasticity of the PIB/SP binary blends were also determined. The results of frequency sweeps and strain sweeps for a particle volume fraction ranging from 0.20 to 0.60 are shown in Fig. S3.

A solid-like linear viscoelastic behavior is well established for $\phi_{SP} \geq 0.30$, where G' marks a plateau while G'' exhibits a local minimum and both moduli increase with ϕ_{SP} . The strain sweeps results show a reduction of the linear viscoelastic domain as ϕ_{SP} increases. Moreover, the G'' overshoot is only observed for $\phi_{SP} \geq 0.30$. Secondary peaks in G'' (almost coinciding with a local maximum in G') are found around $\gamma_0 = 1$ for the highest particle volume fractions ($\phi_{SP} = 0.50$ and 0.60). We note that no $G' - G''$ crossover is found for $\phi_{SP} = 0.60$, but $G' \approx G''$ when $0.1 \lesssim \gamma_0 \lesssim 3$. Such nonlinear behaviors could be due to high particle volume fractions close to the glass transition, where the concept of particle cage breaking could apply¹.

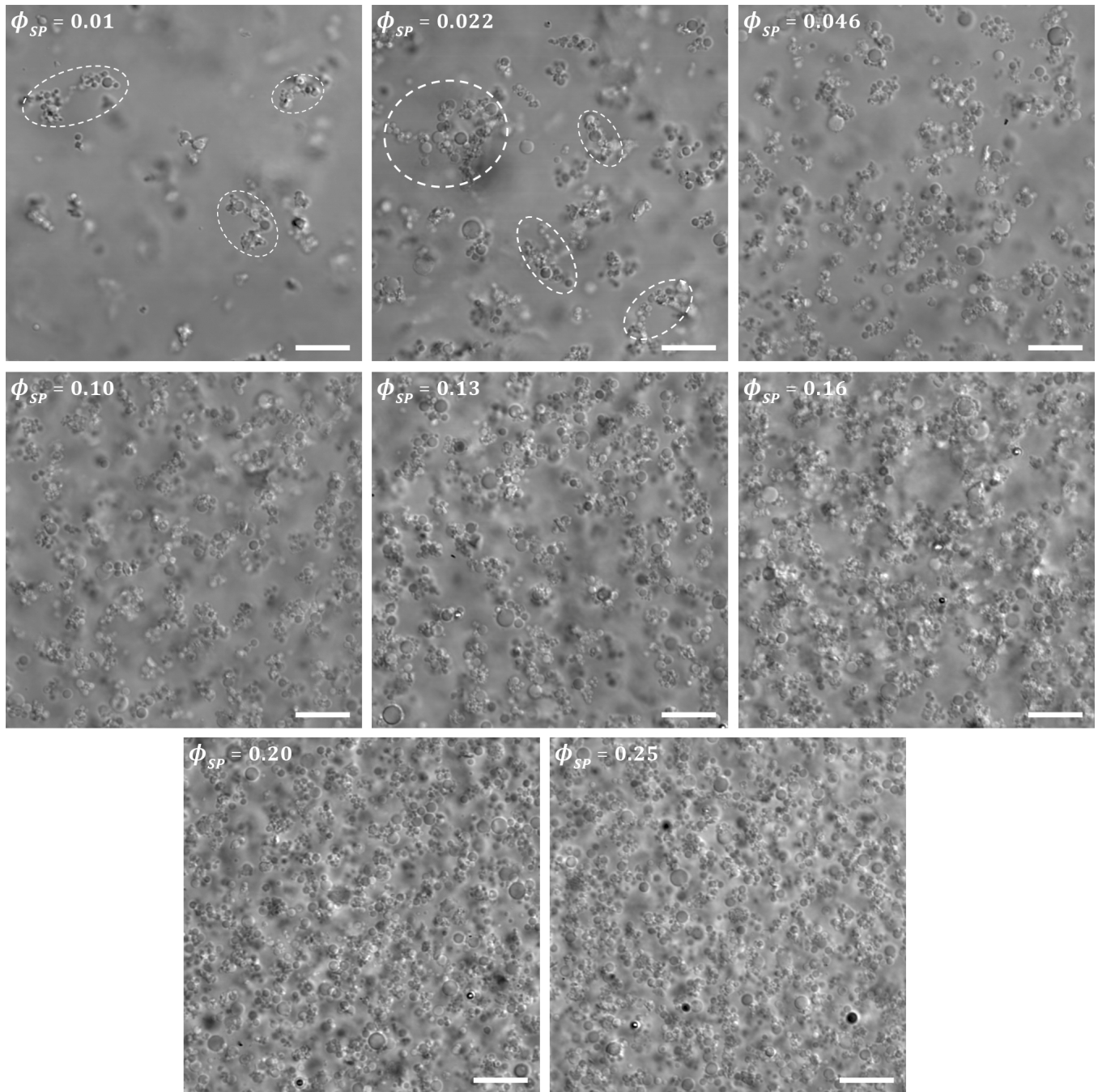


Fig. S2 Differential interference contrast images of pendular gels for a particle volume fraction ϕ_{SP} ranging from 0.01 to 0.25 ($q = 0.16$). Scale bars represent 10 μm . White dashed ellipses surround the isolated pendular flocs observed below the percolation threshold.

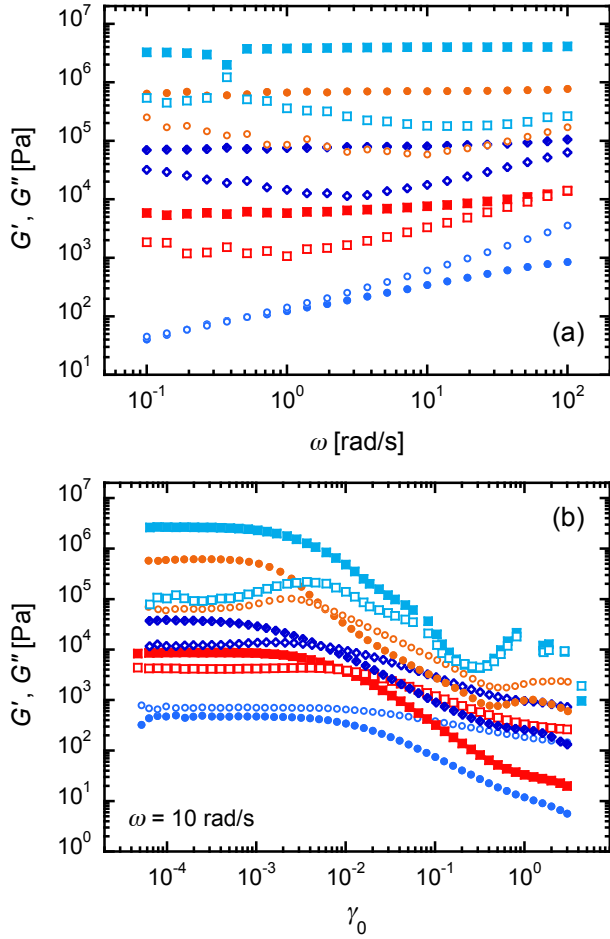


Fig. S3 Dynamic rheological measurements for the PIB/SP binary blends for $\phi_{SP} = 0.20$ (blue circles), 0.30 (red squares), 0.40 (blue diamonds), 0.50 (orange circles) and 0.60 (light blue squares). (a) Frequency sweeps in the linear viscoelastic domain, (b) strain sweeps. G' : filled symbols, G'' : open symbols.

Determining the characteristic relaxation time and shear rate of pendular gels

In the linear domain, the complex viscosity curve of pendular gels exhibits shear-thinning and tends to converge towards a finite value at high frequencies, as represented in Fig. S4a. At low ω , $|\eta^*| = G'_p \omega^{-1}$ while at high ω , $|\eta^*| = \eta_\infty^*$. The characteristic angular frequency ω_c marks the crossover between these two regimes and can thus be defined through the relation $G'_p \omega_c^{-1} = \eta_\infty^*$, i.e. $\omega_c = G'_p / \eta_\infty^*$.

A similar approach is used to define the characteristic shear rate $\dot{\gamma}_c$ for steady state flow curves of pendular gels. For low shear rates, $\sigma = \sigma_y$ while for high shear rates the behavior is Newtonian with $\sigma = \eta_\infty \dot{\gamma}$, as shown in Fig. S4b. The characteristic shear rate $\dot{\gamma}_c$ corresponds to the shear rate value that marks the transition between these two regimes and is defined as $\sigma_y = \eta_\infty \dot{\gamma}_c$, i.e. $\dot{\gamma}_c = \sigma_y / \eta_\infty$.

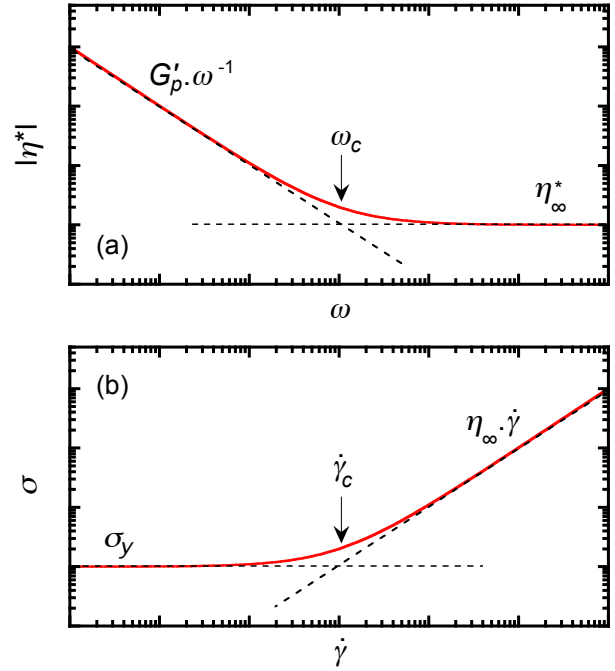


Fig. S4 Representation of (a) the characteristic angular frequency ω_c and (b) the critical shear rate $\dot{\gamma}_c$.

Shear thickening of PIB/PEO/SP ternary systems below the percolation threshold

Non-percolating pendular systems ($\phi_{SP} \lesssim 0.04$) do not have a yield stress. They however exhibit shear thickening, which is directly followed by a shear-thinning regime as shown in Fig. S5. The local maximum in viscosity appears at lower shear rates as ϕ_{SP} increases, similarly to near hard-sphere colloidal suspensions². It is not clear what causes such shear thickening, and why it is observed in the dilute regime. Successive aggregation and breaking of the pendular flocs could be at the origin of the phenomenon.

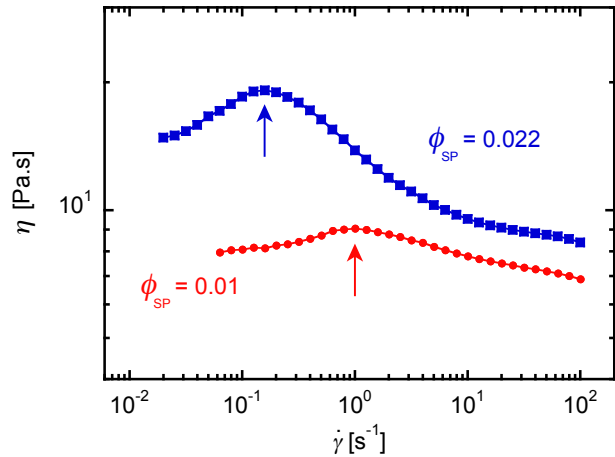


Fig. S5 Steady state flow curves of non-percolating pendular systems.

Scaling of the linear viscoelastic behavior of pendular gels

Dimensionless plot for the G' and G'' spectra of pendular gels is presented in Fig. S6. The master curve obtained using the approach of Trappe and Weitz³ is shown in Fig. S7.

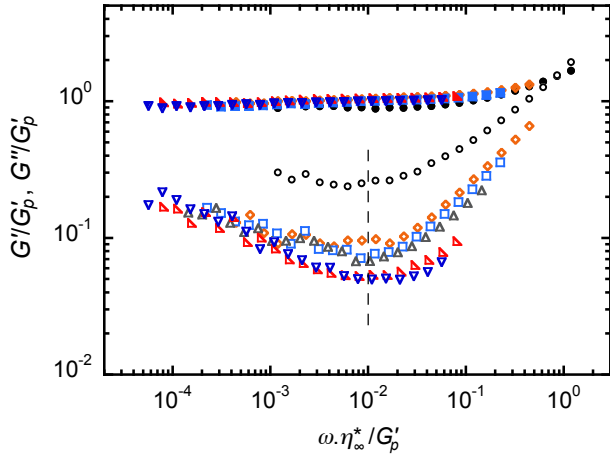


Fig. S6 Dimensionless plot of G' (filled symbols) and G'' (open symbols) for pendular gels, with $\phi_{SP} = 0.10$ (black circles), 0.13 (orange diamonds), 0.16 (blue squares), 0.20 (grey triangles), 0.25 (red tilted triangles) and 0.30 (blue inverted triangles). The dashed line points to the horizontal scaling of the G'' minimum.

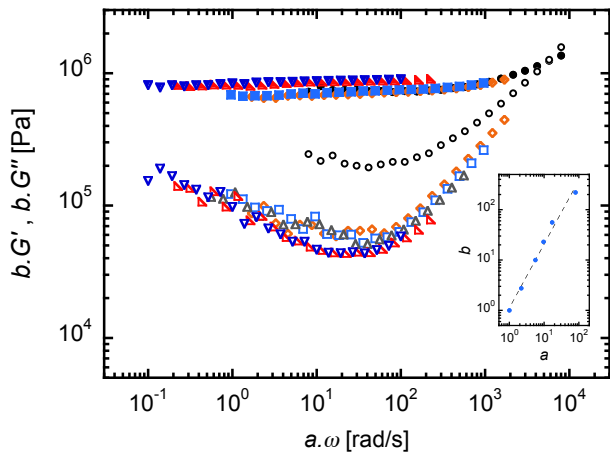


Fig. S7 Master curve for the linear viscoelastic moduli with $\phi_{SP} = 0.30$ as the reference (same symbols as for Fig. S6). Inset shows the shift factors a and b .

Complementary strain sweeps data for pendular gels: stress and elastic stress versus strain

Oscillatory stress-strain curves are shown in Fig. S8. A secondary increase in stress (corresponding to a

weak secondary overshoot in elastic stress $\gamma_0 G'$) is observed for $0.1 \lesssim \gamma_0 \lesssim 3$.

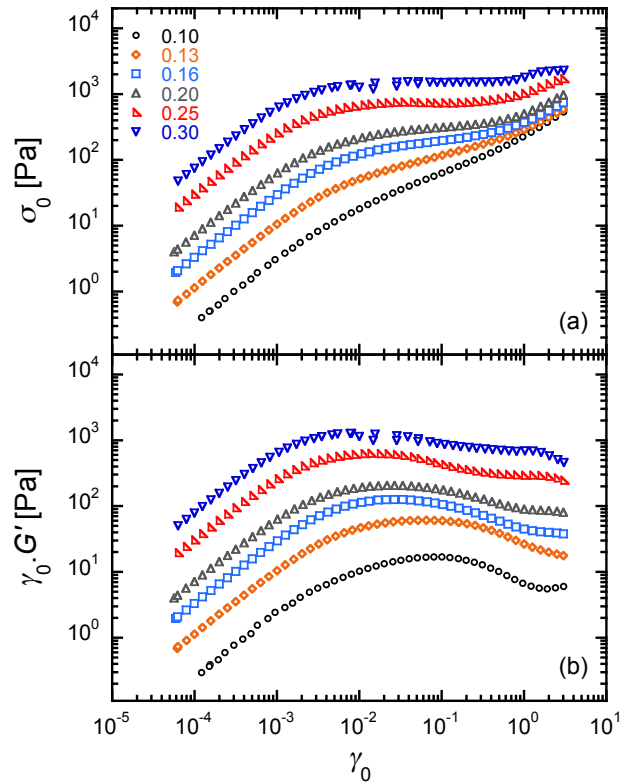


Fig. S8 (a) Stress and (b) elastic stress amplitude vs. strain amplitude during oscillatory strain sweeps for pendular gels. Values of ϕ_{SP} are indicated in the legend.

PEO drops size prior to silica particles addition

Fig. S9 shows PEO drops at the end of the first mixing step. Image analysis yields an average drop radius of $0.6 \mu\text{m}$.

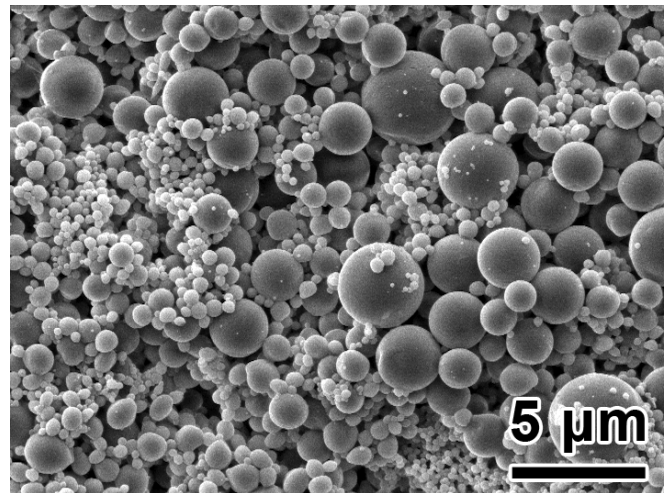


Fig. S9 SEM picture of PEO drops after the first melt-mixing step.

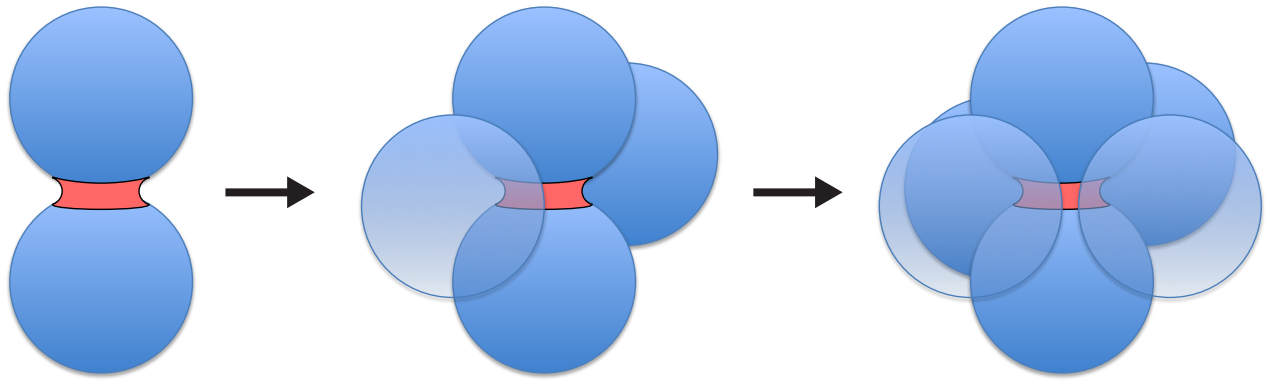


Fig. S10 Scheme of early stages of compact capillary aggregate formation for monodisperse particles. Capillary meniscus in red, particles in blue.

Compact capillary aggregation

Formation of compact capillary aggregates is sketched in Fig. S10 in the case of equal size spherical particles. Starting from a capillary-bridged particles pair, four other particles can join the meniscus when the volume of the latter reaches a critical size.

References

1. N. Koumakis and G. Petekidis, *Soft Matter*, 2011, **7**, 2456–2470.
2. J. Mewis and N. J. Wagner, *Colloidal Suspension Rheology*, Cambridge University Press, 2012.
3. V. Trappe and D. A. Weitz, *Physical Review Letters*, 2000, **85**, 449–452.